

## SYNTHESIS, ANTITUMOR ACTIVITY, PHARMACOPHORE MODELING AND QSAR STUDIES OF NOVEL PYRAZOLES AND PYRAZOLO [1, 5-A] PYRIMIDINES AGAINST BREAST ADENOCARCINOMA MCF-7 CELL LINE

**MAGDA M. F. ISMAIL<sup>a</sup>, DALIA H. SOLIMAN<sup>a</sup>, AMEL M. FARRAG<sup>a\*</sup>, REHAB SABOUR<sup>a</sup>**

**Department of Pharmaceutical Chemistry, Faculty of Pharmacy (Girls), Al-Azhar University, Cairo, Egypt  
Email: amelfarrag@ymail.com**

*Received: 05 Feb 2016 Revised and Accepted: 20 Apr 2016*

### ABSTRACT

**Objective:** The present work aimed to synthesize New series of pyrazoles 3 and pyrazolo[1,5-*a*]pyrimidines 5, 7, 9 in order to evaluate their antiproliferative activity against human breast adenocarcinoma MCF-7 cell line and study the cell cycle progression of the most active compounds. In addition, Pharmacophore modeling and QSAR Studies of these new compounds were done.

**Methods:** The diazonium salt of 4-aminoacetophenone 1 was coupled with malononitrile in ethanol using sodium acetate affords 2-[[4-acetylphenyl]diazonyl] malononitrile. Cycloaddition of hydrazine hydrate, in molar ratios 1:1 or 1:2, on compound 2, furnished 3,5-diaminopyrazole derivatives 3a and 3b respectively. Moreover, new pyrazolo[1,5-*a*]pyrimidine derivatives 5a-f were obtained upon cyclocondensation of 3a, b with different chalcones 4a-c in EtOH/piperidine, while compounds 7a-f were prepared via cycloaddition of 3a, b with various arylidene malononitriles 6a-c in the same reaction condition. Finally, treatment of 3a, b with ethyl 2-cyano-3-ethoxyacrylate 8a or 2-(ethoxymethylene)malononitrile 8b in EtOH/TEA yielded the novel pyrazolo[1,5-*a*]pyrimidine derivatives 9a, b respectively. These target compounds were screened for their cytotoxic activity against MCF-7 (human breast Cell Line) followed by study cell cycle of 7a. Finally, Pharmacophore modeling and QSAR Studies was carried out.

**Results:** The pyrazolopyrimidine 7a was the most active compound (IC<sub>50</sub> = 3.25 μM), whereas, some of the tested compounds exploited moderate growth inhibitory activity. Its effect was further studied on cell cycle progression; results showed that compound 7a induced cell cycle arrest at S-phase verifying this compound as a promising selective anticancer agent.

**Conclusion:** Compound 7a was found to be the most active member against MCF-7 breast cancer (IC<sub>50</sub> = 3.25 μM), Further biological assessment of 7a using flow-cytometric analysis, revealed that it induced cell cycle arrest at S phase.

**Keywords:** Pyrazole, Pyrazolo[1,5-*a*]pyrimidine, MCF-7 breast cancer cell line, Cell cycle profile, 3D pharmacophore, 1 QSAR study

© 2016 The Authors. Published by Innovare Academic Sciences Pvt Ltd. This is an open access article under the CC BY license (<http://creativecommons.org/licenses/by/4.0/>)

### INTRODUCTION

Cancer is one of the most devastating diseases responsible for human loss worldwide. Although there have been great advances in the detection and treatment of cancer, it remains one of the greatest medical challenges [1]. Breast cancer is one of the most common cancers in women. Despite the advances in the treatment of most types of solid tumors (e. g. breast and ovarian cancers) the survival rates are still significantly low [2].

Additionally, chemotherapy in breast cancer treatment has many undesirable side effects. These facts clearly emphasize the need to develop novel effective chemotherapeutic agents [3, 4]. One of the new approaches to cancer therapy is targeting the cell cycle regulation. The cell cycle is controlled and regulated by various mechanisms in mammalian cells. The cell cycle is divided into four phases, G1, S, G2, and M phase. Between these phases are the checkpoints, which control the commitment of the cell to further progress. The two extensively studied checkpoints appear at the G1/S and G2/M boundaries. When checkpoint arrest controls are compromised, this leads to cell cycle dysregulation leading to cancerous cells. Hence, molecules that act as decision makers at these checkpoints are good targets for the cancer treatment [5].

Pyrazole and pyrazolo [1,5-*a*]pyrimidine have emerged as potential pharmacophore scaffolds and have been extensively used to design various antitumor agents (fig. 1). For example, the two aryl pyrazoles in the market, Ruxolitinib (Jakavi®, Novartis) I [6] and Crizotinib (XALKORI®) II [7], (Fig.1), in addition to the N'-(1-[4-nitrophenyl]-3-phenyl-1*H*-pyrazol-4-yl) methylene)-2-chlorobenzohydrazide III which displayed significant activity against MCF-7 cell line [8].

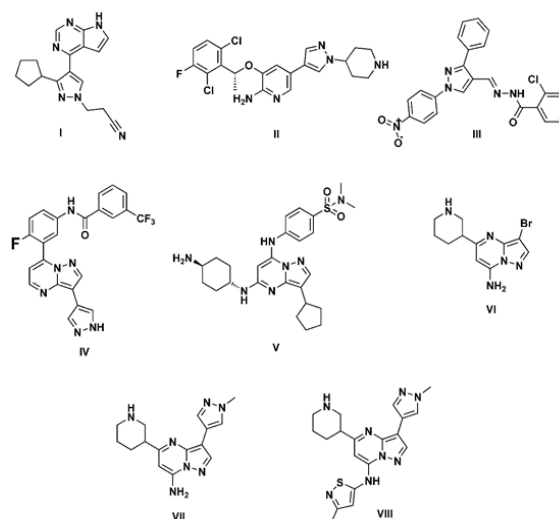


**Fig. 1: Pyrazole and pyrazolo [1,5-*a*] pyrimidine scaffolds based potential candidates and drugs**

Moreover, several pyrazolopyrimidines were effective against different cellular and enzymatic targets involved in dysregulated signaling, for example, the B-Raf kinase inhibitor IV [9] and the cyclin-dependent kinase inhibitor V [10]. It has also been demonstrated that the pyrazolo [1,5-*a*]pyrimidine scaffold itself interacts with the hinge region of many kinase enzymes [11].

Based on these findings and with the attempt to obtain potent anticancer agents the synthesis of new series of pyrazoles and pyrazolo [1,5-*a*] pyrimidines was adopted and evaluated as anticancer agents.

In the present work, position 5 of the pyrazolo[1,5-*a*]pyrimidine scaffold, was replaced by a phenyl moiety, compounds 5a-f, or an amino group, compounds 7a-f, 9a, b, instead of the piperidinyl group in the previously prepared pyrazolopyrimidines VI-VIII. Position 3 was occupied by arylazo moiety whereas position 2 had an amino group in all the series. Finally, generation of a 3D-pharmacophore model and a 2D QSAR model were combined to explore the structural requirements controlling the cytotoxic activities.

## MATERIALS AND METHODS

### General

All chemicals were purchased from VWR International Merck, Germany or Sigma-Aldrich and used without further purification. Melting Points were carried out by open capillary tube method using Stuart SMP3 Melting Point apparatus and they are uncorrected. Elemental Microanalysis was carried out at the Regional Center for Mycology and Biotechnology, Al-Azhar University. Infrared spectra were recorded using potassium bromide discs on Bruker ATR/FTIR Spectrophotometer at the Armed Forces Laboratories. <sup>1</sup>H NMR spectra were recorded on a Varian Gemini 300 MHz Spectrophotometer; the spectra were run at 300 MHz in deuterated dimethyl sulfoxide (DMSO-*d*<sub>6</sub>) at the Armed Forces Laboratories. <sup>13</sup>C NMR Spectra were recorded on a Varian Gemini 300 MHz Spectrophotometer; the spectra were run at 300 and 400 MHz in deuterated dimethyl sulfoxide (DMSO-*d*<sub>6</sub>) at the Armed Forces Laboratories. Chemical shifts were expressed in δ units and were related to that of the solvents. As for the proton magnetic resonance, D<sub>2</sub>O was carried out for NH and OH exchangeable protons. Mass Spectra were recorded using Shimadzu Gas Chromatograph Mass spectrometer-Qp 2010 plus (Japan). All the reactions were followed by TLC using silica gel F254 plates (Merck), and were visualized by UV-lamp. 2-[(4-Acetylphenyl)diazenyl] malononitrile 2 [12], 1,3-diarylprop-2-en-1-ones 4a-c <sup>13</sup>C,2-(substituted benzylidene)-malononitriles 6a-c [14],2-(methoxy methylene) malononitrile 8a and ethyl 2-cyano-3-ethoxyacrylate 8b [15] were prepared according to the previously reported procedures.

### Synthesis

#### Synthesis of 1-(4-[(3,5-Diamino-1H-pyrazol-4-yl) diazenyl] phenylethanone 3a

A mixture of **2** (0.01 mol) and hydrazine hydrate 98% (0.01 mol) was heated in 30 ml ethanol (95%) under reflux for 2 h. The solid product so formed was filtered off and crystallized from ethanol. Yield: 42%; mp 257-260 °C; IR (KBr): 3381, 3268 (NH<sub>2</sub>, NH), 1673 (C=O), 1616 (C=N), 1551 (N=N) cm<sup>-1</sup>; <sup>1</sup>HNMR (300 MHz, DMSO-*d*<sub>6</sub>): δ 2.56 (s, 3H, CH<sub>3</sub>), 6.35 (br. s, 2H, NH<sub>2</sub>, D<sub>2</sub>O-exchangeable), 7.72-7.75 (d, 2H, Ar-H<sub>2,6</sub>, *J* = 8.4 Hz), 7.94-7.96 (d, 2H, Ar-H<sub>3,5</sub>, *J* = 8.4 Hz), 10.80 (s, 1H, NH, D<sub>2</sub>O-exchangeable.); <sup>13</sup>C NMR (400 MHz, DMSO-*d*<sub>6</sub>) δ (ppm): 27.09, 114.79, 120.63, 125.54, 129.73, 134.46, 152.91, 157.40, 197.38; MS [*m/z*, %]: 244 [M<sup>+</sup>, 100]; Anal. calcd. for C<sub>11</sub>H<sub>12</sub>N<sub>6</sub>O (%) : C, 54.09; H, 4.95; N, 34.41. Found: C, 54.22; H, 4.99; N, 34.70.

#### Synthesis of 4-[(4-(1-Hydrazonoethyl)phenyl)diazenyl]-1H-pyrazole -3,5-diamine 3b

A mixture of **2** (0.01 mol) and hydrazine hydrate 98% (0.02 mol) was heated in 30 ml ethanol (95%) under reflux for 2 h. The solid product so formed was filtered off and crystallized from ethanol. Yield: 43%; mp 252-255 °C; IR (KBr): 3398, 3296 (NH<sub>2</sub>, NH), 1614 (C=N), 1589 (N=N)cm<sup>-1</sup>; <sup>1</sup>HNMR (300 MHz, DMSO-*d*<sub>6</sub>) δ: 2.56 (s, 3H, CH<sub>3</sub>), 6.38 (s, 6H, 3NH<sub>2</sub>, D<sub>2</sub>O-exchangeable), 7.73-7.75 (d, 2H, Ar-H<sub>2,6</sub>, *J* = 8.4 Hz), 7.94-7.97 (d, 2H, Ar-H<sub>3,5</sub>, *J* = 8.4 Hz), 10.79 (s, 1H, NH, D<sub>2</sub>O-exchangeable); <sup>13</sup>C NMR (300 MHz, DMSO-*d*<sub>6</sub>) δ (ppm): 26.63, 99.49, 116.64, 120.20, 125.06, 128.60, 129.28, 134.04, 156.82, 156.87, 167.60; MS [*m/z*, %]: 258 [M<sup>+</sup>, 71.27]; Anal. calcd. for C<sub>11</sub>H<sub>14</sub>N<sub>8</sub> (%) : C, 51.31; H, 5.49; N, 43.62. Found: C, 51.15; H, 5.46; N, 43.38.

#### General procedure for the synthesis of pyrazolo [1, 5-*a*] pyrimidines 5a-f

A mixture of equimolar amounts of 3a or 3b and the appropriate substituted chalcones 4a-c were refluxed for 5 h in ethanol (20 ml) containing 3 drops of piperidine. The separated crystalline product was filtered, dried and recrystallized from ethanol.

#### 1-(4-[(2-Amino-7-(4-chlorophenyl)-5-phenylpyrazolo [1,5-*a*]pyrimidin-3-yl)diazenyl] phenylethanone 5a

Yield: 38%; mp 157-160 °C; IR (KBr): 3406, 3296 (NH<sub>2</sub>), 1672 (C=O), 1614 (C=N,N=N) cm<sup>-1</sup>; <sup>1</sup>HNMR (300 MHz, DMSO-*d*<sub>6</sub>) δ: 2.62 (s, 3H, CH<sub>3</sub>), 6.51 (s, 2H, NH<sub>2</sub>, D<sub>2</sub>O-exchangeable), 7.78 (s, 1H, pyrimidine-H), 7.81-8.40 (m, 13H, Ar-H, Ar'-H, Ph-H); <sup>13</sup>C NMR (300 MHz, DMSO-*d*<sub>6</sub>) δ (ppm): 25.73, 88.05, 104.21, 121.00, 125.27, 127.32, 128.32, 128.84, 129.42, 131.68, 135.72, 136.38, 144.31, 147.56, 152.18, 155.89, 197.10; MS [*m/z*, %]: 468 [M<sup>+</sup>+2, 14.57], 466 [M<sup>+</sup>, 40.46]; Anal. calcd. for C<sub>26</sub>H<sub>19</sub>ClN<sub>6</sub>O (%) : C, 66.88; H, 4.10; N, 18.00. Found: C, 67.03; H, 4.14; N, 18.18.

#### 1-(4-[(2-Amino-5-phenyl-7-(*p*-tolyl)pyrazolo[1,5-*a*]pyrimidin-3-yl)diazenyl] phenylethanone 5b

Yield: 50%; mp 153-155 °C; IR (KBr): 3406 (br. NH<sub>2</sub>), 1676 (C=O), 1608 (C=N,N=N) cm<sup>-1</sup>; <sup>1</sup>HNMR (300 MHz, DMSO-*d*<sub>6</sub>): 2.46 (s, 3H, CH<sub>3</sub>), 2.62 (s, 3H, CH<sub>3</sub>-CO), 6.50 (s, 2H, NH<sub>2</sub>, D<sub>2</sub>O-exchangeable), 7.43-7.46 (d, 2H, Ar'-H<sub>3,5</sub>), 7.78 (s, 1H, pyrimidine-H), 7.97-8.39 (m, 11H, Ar-H, Ph-H); <sup>13</sup>C NMR (400 MHz, DMSO-*d*<sub>6</sub>) δ (ppm): 21.57, 27.22, 115.52, 121.47, 121.51, 125.77, 127.86, 128.15, 128.66, 128.88, 129.36, 129.94, 130.21, 130.25, 130.28, 136.99, 140.19, 141.54, 146.04, 152.31, 152.65, 156.70, 197.00; MS [*m/z*, %]: 446 [M<sup>+</sup>, 34.74]; Anal. calcd. for C<sub>27</sub>H<sub>22</sub>N<sub>6</sub>O (%) : C, 76.63; H, 4.97; N, 18.82. Found: C, 72.89; H, 5.08; N, 19.04.

#### 1-(4-[(2-Amino-5-phenyl-7-(3,4,5-trimethoxyphenyl)pyrazolo[1,5-*a*]pyrimidin-3-yl)diazenyl]phenylethanone 5c

Yield: 33%; mp 222-225 °C; IR (KBr): 3412, 3280 (NH<sub>2</sub>), 1676 (C=O), 1622 (C=N,N=N) cm<sup>-1</sup>; <sup>1</sup>HNMR (300 MHz, DMSO-*d*<sub>6</sub>) δ: 2.63 (s, 3H, CH<sub>3</sub>), 3.79 (s, 3H, OCH<sub>3</sub>), 3.91 (s, 6H, 2OCH<sub>3</sub>), 7.09 (s, 2H, NH<sub>2</sub>, D<sub>2</sub>O-exchangeable), 7.44 (s, 2H, NH<sub>2</sub>, D<sub>2</sub>O-exchangeable), 7.54 (s, 2H, H<sub>2,6</sub>, Ar'-H) 7.59-7.80 (m, 5H, Ph-H), 7.96 (s, 1H, pyrimidine-H), 7.98-7.96 (d, 2H, Ar-H<sub>2,6</sub>, *J* = 8.4 Hz), 8.10-8.12 (d, 2H, Ar-H<sub>3,5</sub>, *J* = 8.4 Hz); <sup>13</sup>C NMR (300 MHz, DMSO-*d*<sub>6</sub>) δ (ppm): 26.67, 48.98, 56.26, 60.12, 106.37, 107.82, 107.93, 116.17, 121.02, 125.42, 127.41, 128.88, 129.43, 130.76, 135.65, 136.32, 139.79, 145.57, 147.98, 152.10, 152.55, 155.95, 156.61, 197.07; MS [*m/z*, %]: 522 [M<sup>+</sup>, 26.31]; Anal. calcd. for C<sub>29</sub>H<sub>26</sub>N<sub>6</sub>O<sub>4</sub> (%) : C, 66.66; H, 5.02; N, 16.08. Found: C, 66.89; H, 5.11; N, 16.31.

#### 7-(4-Chlorophenyl)-3-[(4-(1-hydrazonoethyl)phenyl)diazenyl]-5-phenylpyrazolo[1,5-*a*]pyrimidin-2-amine 5d

Yield: 28%; mp 220-222 °C; IR (KBr): 3417, 3377(2NH<sub>2</sub>), 1614 (C=N,N=N) cm<sup>-1</sup>; <sup>1</sup>HNMR (300 MHz, DMSO-*d*<sub>6</sub>) δ: 2.05 (s, 3H, CH<sub>3</sub>), 6.40 (s, 2H, NH<sub>2</sub>, D<sub>2</sub>O-exchangeable), 6.49 (s, 2H, NH<sub>2</sub>, D<sub>2</sub>O-exchangeable), 7.27-7.46 (m, 3H, Ph-H), 7.58-7.80 (m, 7H, 2 Ph-H, 4Ar-H) & pyrimidine-H), 8.22-8.25 (d, 2H, Ar-H<sub>2,6</sub>), 8.38-8.42 (d, 2H, Ar-H<sub>3,5</sub>); <sup>13</sup>C NMR (400 MHz, DMSO-*d*<sub>6</sub>) δ (ppm): 11.74, 58.82, 115.52, 121.50, 125.77, 126.61, 127.82, 128.95, 129.30, 129.38, 129.87, 131.21, 132.19, 132.70, 136.23, 136.88, 141.73, 142.08, 144.82, 147.90, 152.27, 156.77; MS [*m/z*, %]: 482 [M<sup>+</sup>+2, 31.11], 480 [M<sup>+</sup>, 24.78]; Anal. calcd. for C<sub>26</sub>H<sub>21</sub>ClN<sub>8</sub> (%) : C, 64.93; H, 4.40; N, 23.30. Found: C, 65.08; H, 4.46; N, 23.45.

#### 3-[(4-(1-Hydrazonoethyl)phenyl)diazenyl]-5-phenyl-7-(*p*-tolyl)pyrazolo[1,5-*a*]pyrimidin-2-amine 5e

Yield: 40%; mp 185-190 °C; IR (KBr): 3379, 3278 (NH<sub>2</sub>), 1616 (C=N,N=N) cm<sup>-1</sup>; <sup>1</sup>HNMR (300 MHz, DMSO-*d*<sub>6</sub>) δ: 2.28 (s, 3H, CH<sub>3</sub>), 2.38 (s, 3H, N=C-CH<sub>3</sub>), 6.49 (s, 2H, NH<sub>2</sub>, D<sub>2</sub>O-exchangeable), 7.19-7.22 (d, 2H, Ar'-H<sub>3,5</sub>), 7.28 (s, 2H, NH<sub>2</sub>, D<sub>2</sub>O-exchangeable), 7.40-7.46 (m, 3H, Ph-H), 7.58-7.80 (m, 5H, 2 Ar-H<sub>2,6</sub>+2 Ar'-H<sub>2,6</sub>+pyrimidine-H), 8.11-8.14 (d, 2H, Ph-H), 8.39-8.42 (m, 2H, Ar-H<sub>3,5</sub>); <sup>13</sup>C NMR (300 MHz, DMSO-*d*<sub>6</sub>) δ (ppm): 11.22, 26.54, 58.82, 101.34, 120.19, 124.86,

125.09, 128.34, 128.75, 129.03, 129.39, 129.89, 131.21, 132.19, 132.70, 136.23, 137.92, 141.84, 144.72, 147.00, 152.41, 168.00; MS [*m/z*, %]: 461 [*M*<sup>+</sup>+1, 4.29]; Anal. calcd. for C<sub>27</sub>H<sub>24</sub>N<sub>8</sub> (%) : C, 70.42; H, 5.25; N, 24.33. Found: C, 70.60; H, 5.29; N, 24.47.

### 3-[(4-(1-Hydranoethyl)phenyl)diazanyl]-5-phenyl-7-(3,4,5-trimethoxyphenyl) pyrazolo[1,5-a]pyrimidin-2-amine 5f

Yield: 35%; mp 138-140 °C; IR (KBr): 3293 (br. 2NH<sub>2</sub>), 1600 (C=N,N=N) cm<sup>-1</sup>; <sup>1</sup>HNMR (300 MHz, DMSO-d<sub>6</sub>) δ: 2.34 (s, 3H, CH<sub>3</sub>), 3.79 (s, 3H, OCH<sub>3</sub>), 3.91 (s, 6H, 2OCH<sub>3</sub>), 6.53 (s, 2H, NH<sub>2</sub>, D<sub>2</sub>O-exchangeable), 7.44 (s, 2H, NH<sub>2</sub>, D<sub>2</sub>O-exchangeable), 7.54 (s, 2H, Ar<sup>-</sup>-H<sub>2</sub>, δ), 7.49-7.62 (m, 9H, Ar-H, Ph-H), 8.41 (s, 1H, pyrimidine-H); <sup>13</sup>C NMR (300 MHz, DMSO-d<sub>6</sub>) δ (ppm): 26.78, 56.25, 56.31, 71.20, 106.49, 107.80, 107.97, 116.17, 121.04, 125.44, 127.41, 128.94, 129.45, 135.66, 136.33, 145.58, 147.98, 152.11, 152.57, 155.95, 156.63, 197.09; MS [*m/z*, %]: 536 [*M*<sup>+</sup>, 8.89]; Anal. calcd. for C<sub>29</sub>H<sub>28</sub>N<sub>8</sub>O<sub>3</sub> (%) : C, 64.91; H, 5.26; N, 20.88. Found: C, 65.12; H, 5.30; N, 21.09.

### General procedure for the synthesis of pyrazolo [1, 5-a] pyrimidines 7a-f

Equivalent amounts of **3a** or **3b** and appropriate arylidene-malononitriles **6a-c** were heated under reflux in ethanol (20 ml) and piperidine (3-4 drops) for 4 h, pyrazolo[1,5-a]pyrimidines were precipitated on hot, filtered, dried and crystallized from absolute ethanol.

### 3-[(4-Acetylphenyl)diazanyl]-2,5-diamino-7-(4-chlorophenyl) pyrazolo[1,5a]pyrimidine-6-carbonitrile 7a

Yield: 48%, mp 227-230 °C; IR (KBr): 3402, 3302 (2NH<sub>2</sub>), 2212 (CN), 1660 (C=O), 1616 (C=N,N=N) cm<sup>-1</sup>; <sup>1</sup>HNMR (300 MHz, DMSO-d<sub>6</sub>) δ: 2.60 (s, 3H, CH<sub>3</sub>), 7.23 (s, 2H, NH<sub>2</sub>, D<sub>2</sub>O-exchangeable), 7.67-7.74 (m, 4H, Ar<sup>-</sup>-H), 7.90-8.15 (m, 4H, 4-Cl-Ar-H), 8.67 (s, 2H, NH<sub>2</sub>, D<sub>2</sub>O-exchangeable); <sup>13</sup>C NMR (300 MHz, DMSO-d<sub>6</sub>) δ (ppm): 26.64, 117.64, 120.13, 127.42, 128.53, 129.75, 130.43, 134.02, 134.96, 136.05, 148.79, 151.91, 154.97, 155.57, 156.86, 186.77, 197.36; MS [*m/z*, %]: 432 [*M*<sup>+</sup>+2, 1.07], 430 [*M*<sup>+</sup>, 1.31]; Anal. calcd. for C<sub>21</sub>H<sub>15</sub>ClN<sub>8</sub>O (%) : C, 58.54; H, 3.51; N, 26.01. Found: C, 58.71 H, 3.49; N, 26.28.

### 3-[(4-Acetylphenyl)diazanyl]-2,5-diamino-7-(4-methoxyphenyl) pyrazolo[1,5-a]pyrimidine-6-carbonitrile 7b

Yield: 57%; mp 162-165 °C; IR (KBr): 3398, 3300 (2NH<sub>2</sub>), 2210 (CN), 1674 (C=O), 1614 (C=N, N=N) cm<sup>-1</sup>; <sup>1</sup>HNMR (300 MHz, DMSO-d<sub>6</sub>) δ: 2.57 (s, 3H, CH<sub>3</sub>), 3.87 (s, 3H, OCH<sub>3</sub>), 7.12-7.14 (d, 2H, Ar<sup>-</sup>-H<sub>3,5</sub>), 7.18 (s, 2H, NH<sub>2</sub>, D<sub>2</sub>O-exchangeable), 7.21 (s, 2H, NH<sub>2</sub>, D<sub>2</sub>O-exchangeable), 7.86-7.89 (m, 2H, H<sub>2,6</sub>, Ar<sup>-</sup>-H), 7.95-7.97 (d, 2H, Ar-H<sub>2,6</sub>, *J* = 8.4 Hz), 8.08-8.06 (d, 2H, Ar-H<sub>3,5</sub>, *J* = 8.4 Hz); <sup>13</sup>C NMR (400 MHz, DMSO-d<sub>6</sub>) δ (ppm): 27.08, 55.86, 76.18, 114.20, 116.78, 118.06, 120.72, 121.61, 127.60, 129.91, 130.88, 136.40, 147.13, 149.44, 152.40, 156.14, 157.36, 161.55, 197.36; MS [*m/z*, %]: 426 [*M*<sup>+</sup>, 72.60]; Anal. calcd. for C<sub>22</sub>H<sub>18</sub>N<sub>8</sub>O<sub>2</sub> (%) : C, 61.96; H, 4.25; N, 26.28. Found: C, 62.08; H, 4.31; N, 26.57.

### 3-[(4-Acetylphenyl) diazanyl]-2,5-diamino-7-(2,3-dimethoxyphenyl)pyrazolo[1,5-a]pyrimidine-6-carbonitrile 7c

Yield: 48%; mp 225-227 °C; IR (KBr): 3450, 3340 (2NH<sub>2</sub>), 2233 (CN), 1674 (C=O), 1614 (C=N), 1589 (N=N) cm<sup>-1</sup>; <sup>1</sup>HNMR (300 MHz, DMSO-d<sub>6</sub>) δ: 2.59 (s, 3H, CH<sub>3</sub>), 3.74 (s, 3H, OCH<sub>3</sub>), 3.89 (s, 3H, OCH<sub>3</sub>), 7.0-7.23 (m, 3H, Ar<sup>-</sup>-H), 7.86-7.89 (d, 2H, Ar-H<sub>2,6</sub>, *J* = 8.4 Hz), 8.02-8.05 (d, 2H, Ar-H<sub>3,5</sub>, *J* = 8.4 Hz), 8.60 (s, 2H, NH<sub>2</sub>, D<sub>2</sub>O-exchangeable); <sup>13</sup>C NMR (300 MHz, DMSO-d<sub>6</sub>) δ (ppm): 26.66, 55.85, 78.69, 115.18, 121.22, 129.39, 132.16, 136.05, 148.01, 147.00, 151.91, 152.29, 155.57, 197.11; MS [*m/z*, %]: 456 [*M*<sup>+</sup>, 6.01]; Anal. calcd. for C<sub>23</sub>H<sub>20</sub>N<sub>8</sub>O<sub>3</sub> (%) : C, 60.52; H, 4.42; N, 24.55. Found: C, 60.74; H, 4.49; N, 24.69.

### 2,5-Diamino-7-(4-chlorophenyl)-3-[(4-(1-hydranoethyl) phenyl)diazanyl]pyrazolo[1,5-a] pyrimidine-6-carbonitrile 7d

Yield: 34%; mp 215-220 °C; IR (KBr): 3396, 3296, 3184 (3NH<sub>2</sub>), 2208 (CN), 1614(C=N),1595 (N=N) cm<sup>-1</sup>; <sup>1</sup>HNMR (300 MHz, DMSO-d<sub>6</sub>) δ: 2.41 (s, 3H, CH<sub>3</sub>), 6.34 (s, 2H, NH<sub>2</sub>, D<sub>2</sub>O-exchangeable), 7.55-7.58 (d, 2H, Ar<sup>-</sup>-H<sub>2,6</sub>, *J* = 8.4 Hz), 7.63-7.66 (d, 2H, Ar<sup>-</sup>-H<sub>3,5</sub>, *J* = 8.4 Hz), 7.71-7.74 (d, 2H, Ar-H<sub>2,6</sub>, *J* = 8.4 Hz), 7.89-7.92 (d, 2H, Ar-H<sub>3,5</sub>, *J* = 8.4

Hz), 10.76 (s, 2H, NH<sub>2</sub>, D<sub>2</sub>O-exchangeable); <sup>13</sup>C NMR (300 MHz, DMSO-d<sub>6</sub>) δ (ppm): 14.75, 115.19, 120.15, 126.88, 127.45, 128.87, 129.72, 133.33, 134.97, 147.00, 148.61, 152.03, 153.47, 154.97, 156.41, 163.80, 169.00; MS [*m/z*, %]: 446 [*M*<sup>+</sup>+2, 0.47], 444 [*M*<sup>+</sup>, 1.13]; Anal. calcd. for C<sub>21</sub>H<sub>17</sub>ClN<sub>10</sub> (%) : C, 56.70; H, 3.85; N, 31.48. Found: C, 56.87; H, 3.92; N, 31.67.

### 2,5-Diamino-3-[(4-(1-hydranoethyl)phenyl)diazanyl]-7-(4-methoxyphenyl)pyrazolo[1,5-a]pyrimidine-6-carbonitrile 7e

Yield: 41%; mp 190-192 °C; IR (KBr): 3427, 3303, 3223 (3NH<sub>2</sub>), 2199 (CN), 1605 (C=N,N=N) cm<sup>-1</sup>; <sup>1</sup>HNMR (300 MHz, DMSO-d<sub>6</sub>) δ: 2.50 (s, 3H, CH<sub>3</sub>), 3.83 (s, 2H, NH<sub>2</sub>, D<sub>2</sub>O-exchangeable), 3.87 (s, 3H, OCH<sub>3</sub>), 7.08-8.63 (m, 8H, Ar-H); <sup>13</sup>C NMR (300 MHz, DMSO-d<sub>6</sub>) δ (ppm): 22.49, 55.30, 87.80, 113.76, 114.38, 117.06, 121.12, 126.98, 127.58, 128.58, 130.40, 148.91, 153.77, 157.91, 160.45, 161.55, 162.90, 169.9; MS [*m/z*, %]: 439 [*M*<sup>+</sup>-1, 4.28]; Anal. calcd. for C<sub>22</sub>H<sub>20</sub>N<sub>10</sub>O (%) : C, 59.99; H, 4.58; N, 31.80. Found: C, 60.17; H, 4.66; N, 32.07.

### 2,5-Diamino-7-(2,3-dimethoxyphenyl)-3-[(4-(1-hydranoethyl) phenyl)diazanyl] pyrazolo[1,5-a] pyrimidine-6-carbonitrile 7f

Yield: 48%; mp 288-290 °C; IR (KBr): 3392, 3298, 3168 (3NH<sub>2</sub>), 2179 (CN) cm<sup>-1</sup>; <sup>1</sup>HNMR (300 MHz, DMSO-d<sub>6</sub>) δ: 2.34 (s, 3H, CH<sub>3</sub>), 3.83, 3.86 (2s, 6H, 2OCH<sub>3</sub>), 6.21 (s, 2H, NH<sub>2</sub>, D<sub>2</sub>O-exchangeable), 7.63 (m, 3H, Ar<sup>-</sup>-H), 7.72-7.75 (d, 2H, Ar-H<sub>2,6</sub>, *J* = 8.4 Hz), 7.97-7.94 (d, 2H, Ar-H<sub>3,5</sub>, *J* = 8.4 Hz), 10.75 (s, 2H, NH<sub>2</sub>, D<sub>2</sub>O-exchangeable); <sup>13</sup>C NMR (300 MHz, DMSO-d<sub>6</sub>) δ (ppm): 14.64, 66.3, 114.99, 120.16, 125.06, 127.13, 127.45, 135.64, 154.53, 157.56; MS [*m/z*, %]: 470 [*M*<sup>+</sup>, 4.16]; Anal. calcd. for C<sub>23</sub>H<sub>22</sub>N<sub>10</sub>O<sub>2</sub> (%) : C, 58.71; H, 4.71; N, 29.77. Found: C, 58.97; H, 4.76; N, 29.8.

### General procedure for the synthesis of pyrazolo[1,5-a]pyrimidines 9a, b

Equimolar amounts of **3a** and ethyl 2-cyano-3-ethoxyacrylate **8a** or **3b** and ethoxymethylenemalononitrile **8b** were heated under reflux for 6 h in ethanol (20 ml) and 5 drops of triethylamine. The precipitate was filtered on hot, dried and crystallized from ethanol.

### Ethyl3-[(4-acetylphenyl) diazanyl]-2,5-diaminopyrazolo[1,5-a]pyrimidine-6-carboxylate 9a

Yield: 45%, mp 291-293 °C; IR (KBr): 3425, 3309 (2NH<sub>2</sub>), 1720 (C=O ester),1670 (C=O),1616 (C=N),1589 (N=N) cm<sup>-1</sup>; <sup>1</sup>HNMR (300 MHz, DMSO-d<sub>6</sub>) δ: 1.33-1.37 (t, 3H, CH<sub>2</sub>CH<sub>3</sub>), 2.61 (s, 3H, CH<sub>3</sub>), 4.34-4.37 (q, 4H, CH<sub>2</sub>CH<sub>3</sub>), 7.18 (s, 2H, NH<sub>2</sub>, D<sub>2</sub>O-exchangeable), 7.88-8.09 (m, 4H, Ar-H), 8.69 (s, 1H, pyrimidine-H); <sup>13</sup>C NMR (400 MHz, DMSO-d<sub>6</sub>) δ (ppm): 14.67, 27.25, 61.18, 110.00, 121.63, 127.02, 127.12, 129.93, 136.47, 147.83, 152.24, 152.79, 156.14, 161.50, 197.00; MS [*m/z*, %]: 367 [*M*<sup>+</sup>, 1.75]; Anal. calcd for C<sub>17</sub>H<sub>17</sub>N<sub>7</sub>O<sub>3</sub> (%) : C, 55.58; H, 4.66; N, 26.69. Found: C, 55.81; H, 4.69; N, 26.78.

### 2,5-Diamino-3-(4-(1-hydranoethyl) phenyl) diazanyl) pyrazolo[1,5-a]pyrimidine-6-carbonitrile 9b

Yield: 55%, mp 293-295 °C; IR (KBr): 3396, 3302, 3265 (2NH<sub>2</sub>), 2214 (CN), 1612 (C=N,N=N) cm<sup>-1</sup>; <sup>1</sup>HNMR (300 MHz, DMSO-d<sub>6</sub>) δ: 2.34 (s, 3H, CH<sub>3</sub>), 6.38 (s, 2H, NH<sub>2</sub>, D<sub>2</sub>O-exchangeable), 7.64 (s, 1H, pyrimidine-H), 7.75-7.97 (m, 4H, Ar-H), 10.79 (s, 4H, 2NH<sub>2</sub>, D<sub>2</sub>O-exchangeable); <sup>13</sup>C NMR (300 MHz, DMSO-d<sub>6</sub>) δ (ppm): 14.64, 66.95, 115.00, 120.18, 121.13, 127.09, 127.42, 135.63, 147.84, 151.80, 154.53, 157.56, 168.26; MS [*m/z*]: 334 [*M*<sup>+</sup>, 5.91]; Anal. calcd. for C<sub>15</sub>H<sub>14</sub>N<sub>10</sub> (%) : C, 53.89; H, 4.22; N, 41.89. Found: C, 54.08; H, 4.26; N, 42.13.

### Biological assay

#### Cell culture

Cancer cells from breast cancer cell line (MCF-7, human breast adenocarcinoma) was purchased from American type Cell Culture collection (ATCC, Manassas, USA) and grown on the appropriate growth medium Dulbecco's modified Eagle's medium (DMEM) or Roswell Park Memorial Institute medium (RPMI 1640) supplemented with 100 mg/ml of streptomycin, 100 units/ml of penicillin and 10% of heat-inactivated fetal bovine serum in a humidified, 5% (v/v) CO<sub>2</sub> atmosphere at 37 °C.

### Cell growth inhibitory assay

Cytotoxicity was determined using 3-[4,5-dimethylthiazole-2-yl]-2,5-diphenyltetrazolium bromide (MTT) method. Exponentially growing cells were trypsinized, counted and seeded at the appropriate densities (2000-1000 cells/0.33 cm<sup>2</sup> well) into 96-well microtiter plates. Cells then were incubated in a humidified atmosphere at 37°C for 24 h. Then, cells were exposed to different concentrations of compounds (0.1, 10, 100, 1000 μM) for 72 h. Then the viability of treated cells was determined using MTT technique as follow. Media were removed; cells were incubated with 200 μl of 5% MTT solution/well (Sigma-Aldrich, MO) and were allowed to metabolize the dye into colored-insoluble formazan crystals for 2 h. The remaining MTT solution was discarded from the wells, and the formazan crystals were dissolved in 200 μl/well-acidified isopropanol for 30 min, covered with aluminum foil and with continuous shaking using a MaxQ 2000 plate shaker (Thermo Fisher Scientific Inc, MI) at room temperature. Absorbances were measured at 570 nm using a Stat FaxR 4200 plate reader (Awareness Technology, Inc., FL). The cell viability was expressed as a percentage of control and the concentration that induces 50% of maximum inhibition of cell proliferation (IC<sub>50</sub>) were determined using Graph Pad Prism version 5 software (Graph Pad software Inc, CA) [16, 17].

### Cell cycle analysis (DNA-Flow Cytometry Analysis)

MCF-7 cells at a density of 4 x10<sup>6</sup> cell by T 75 flasks were exposed to (Compound X) at its IC<sub>50</sub> for 24 h. The cells then were collected by trypsinization, washed in PBS and fixed in absolute ice-cold alcohol. Thereafter, cells were stained using Cycle TEST™ PLUS DNA Reagent Kit (BD Biosciences, San Jose, CA) according to the manufacturer's instructions. Cell-cycle distribution was determined using a FACS Caliber flow cytometer (BD Biosciences, San Jose, CA).

### Datasets

All molecular modeling studies (3D-QSAR and pharmacophore model) were performed using the molecular modeling software package DS 2.5 software (Discovery Studio 2.5, Accelrys, Co. Ltd).

A dataset of 16 of the synthesized compounds was used as a training set with their inhibitory activities in IC<sub>50</sub> (μM) was used in present study.

### Development of QSAR model

A set of 13 of the synthesized compounds was used as a training set for the QSAR modeling. This test set displayed variable anticancer activities representing potent, moderate and weak anticancer activity. The most active compound 7a along with one of the moderate 5d and one of the week compounds 3b were used as statistical outliers. Molecular descriptors were calculated for each compound employing a "Calculate Molecular Properties" module

which used for calculating different molecular properties for the training set compounds. 2D Descriptors involved: AlogP, molecular property counts, surface area and volume and topological descriptors while the 3D descriptors involved: Dipole, jurs descriptors, principle moments of inertia, shadow indices, and surface area and volume was employed. Genetic function approximation (GFA) was utilized to search for the best possible QSAR regression equation capable of correlating the variations in the biological activities of the training compounds with variations in the generated descriptors, *i.e.*, multiple linear regression modeling (MLR). Different descriptors such as ES\_Sum\_dsN (Calculates the sums of the Electrotopological State (E-state) values of each atom type), Dipole\_mag (3D electronic descriptors that indicates the strength and orientation behavior of a molecule in an electrostatic field), Jurs\_WNSA\_3 (the surface-weighted charged partial surface areas "set of six descriptors" (Jurs\_WPSA\_1, Jurs\_WPSA\_2, Jurs\_WPSA\_3, Jurs\_WNSA\_1, Jurs\_WNSA\_2 and Jurs\_WNSA\_3) obtained by multiplying descriptors 1 to 6 by the total molecular solvent-accessible surface area and dividing by 1000, Jurs descriptors are those ones that combine shape and electronic information to characterize molecules) were utilized in the models generated. Experimental anticancer activities, measured as IC<sub>50</sub> in μM were used for the QSAR modeling.

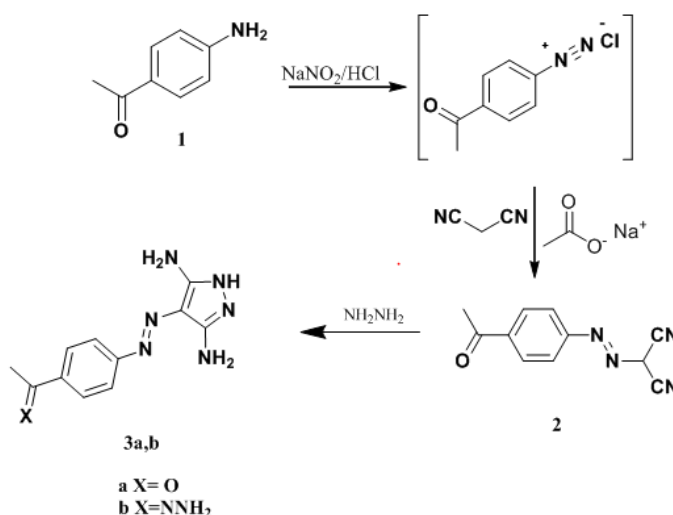
The QSAR model was validated employing leave-one-out cross-validation by setting the folds to a number much larger than the number of samples, r<sup>2</sup> (squared correlation coefficient value) and r<sup>2</sup> prediction (predictive squared correlation coefficient value) [18], residuals between the predicted and experimental activity of the test set and training set. Statistical outliers were identified from experimental versus predicted plots.

### Pharmacophore modeling

The 3D-QSAR Pharmacophore Generation protocol (Catalyst HypoGen algorithm) was used to derive structure-activity relationship hypothesis models (3D-QSAR pharmacophore models). HypoGen identifies features common to the active compounds and excludes features common to the inactive ones within conformationally allowable regions of space. It further estimates the activity of the newly synthesized and tested compounds using regression parameters. Thus, a training set of the 16 synthesized compounds were used in this study to construct a pharmacophore model using hydrogen bond acceptor (HBA), hydrogen bond donor (HBD), hydrophobic (H), ring aromatic (RA) and positive ionizable (Poslon) chemical features.

### RESULTS AND DISCUSSION

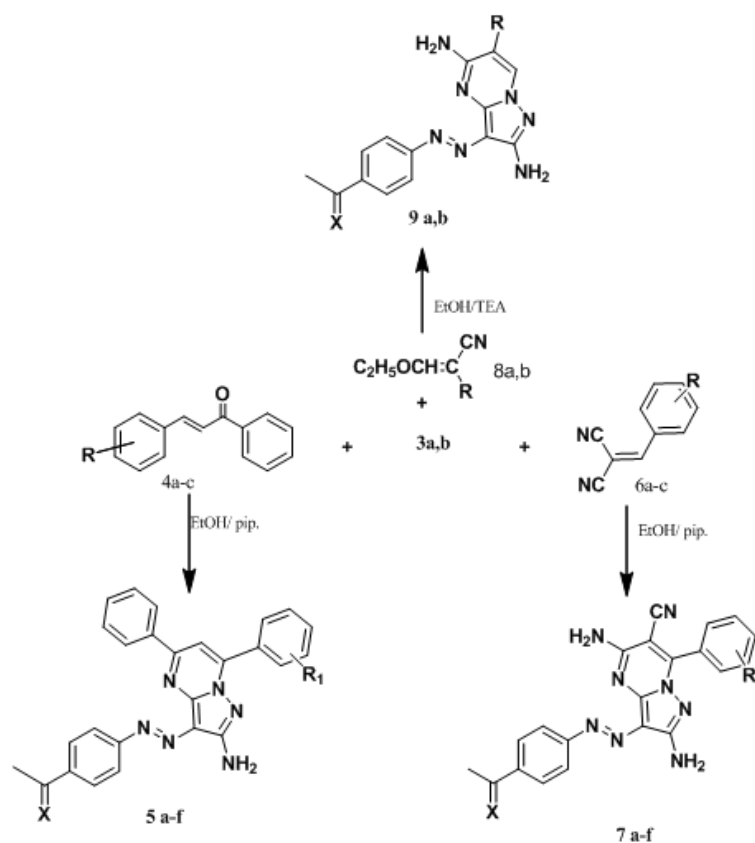
The route adopted for the preparation of target pyrazoles 3 and pyrazolo[1,5-a]pyrimidine derivatives 5, 7 and 9 are depicted in Schemes 1 and 2 respectively.



Scheme 1: Synthesis of compounds 3a, b

The diazonium salt of 4-aminoacetophenone **1** was coupled with malononitrile in ethanol using sodium acetate, [12, 19-23] to afford 2-[(4-acetylphenyl)diazenyl] malononitrile **2** [12]. Cycloaddition of compound **2** with hydrazine hydrate in molar ratios 1:1 [20-24] or 1:2, furnished 3,5-diaminopyrazole derivatives **3a** and **3b** respectively. The structures of **3a,b** were well established from their microanalytical and spectral data. The IR spectrum of **3a** revealed the appearance of two NH<sub>2</sub> and NH at  $\lambda_{\max}$  3381 and 3268 cm<sup>-1</sup> with the lack of CN band of the parent **2**. Its <sup>1</sup>HNMR spectrum (DMSO-d<sub>6</sub>) showed two singlet at  $\delta$  6.35 and 10.80 ppm corresponding to NH<sub>2</sub> and NH (exchangeable with D<sub>2</sub>O). Moreover, new pyrazolo [1,5-*a*]pyrimidine derivatives **5a-f** were obtained upon cyclocondensation of **3a, b** with different chalcones **4a-c** in EtOH/pip. [25], while compounds **7a-f** were prepared via cycloaddition [19] of **3a, b** with various arylidene malononitriles **6a-c** in the same reaction condition. Finally treatment of **3a, b** with ethyl 2-cyano-3-ethoxyacrylate **8a** or 2-(ethoxymethylene) malononitrile

**8b** in EtOH/TEA [19, 26] yielded the novel pyrazolo[1,5-*a*]pyrimidine derivatives **9a, b** respectively. Elemental and spectral analysis of **5a-f**, **7a-f** and **9a, b** were in agreement with their structures. Compound **5b** displayed the appearance of two singlet at  $\delta$  2.46 and 2.62 ppm corresponding to two methyl protons and showed characteristic singlet for pyrimidine-H at  $\delta$  7.78 ppm. In addition its <sup>13</sup>C NMR spectrum showed 2 singlet at  $\delta$  21.57 and 27.22 ppm corresponding to two methyl groups. The IR spectrum of **7b** revealed a new band for CN at  $\lambda_{\max}$  2210, while its <sup>1</sup>HNMR spectrum (DMSO-d<sub>6</sub>) showed singlet at  $\delta$  3.87 ppm corresponding to three protons of the OCH<sub>3</sub> group. **9a** IR spectrum demonstrated a band at 1670 cm<sup>-1</sup> related to carbonyl ester in addition to the band at 1720 cm<sup>-1</sup> corresponding to acetyl C=O. Its <sup>1</sup>HNMR spectra showed the characteristic triplet and quartet signals attributed to the ethyl protons in the region of 1.33-1.37 and 4.34-4.37 respectively, in addition to signal at  $\delta$  8.69 ppm attributed to pyrimidine-H.



Scheme 2: Synthesis of compounds **5, 7, 9**

### Antitumor properties

The *in vitro* antitumor activity against human breast cancer cells (MCF-7) of the 16 test compounds was achieved in the cell culture lab, College of Pharmacy, Al-Azhar University, Cairo, Egypt. Doxorubicin was used as a reference standard, and it showed IC<sub>50</sub> = 2.008  $\mu$ M.

The anticancer MCF-7 profile suggested that the test compounds showed variable activities compared to reference drug as shown in (table 1).

It was observed that the 3, 5-diaminopyrazole **3a** bearing a C=O group showed about 42 times the anticancer activity of its counterpart **3b** (IC<sub>50</sub> = 26.2, 1083.30  $\mu$ M, respectively) which bears a C=NNH<sub>2</sub> group instead. Additionally **3a** was found to be approximately 1.27 times more potent than 4-[(3,5-diamino-1H-pyrazol-4-yl)diazenyl]phenol (IC<sub>50</sub> = 33  $\mu$ M)[20]. Similarly, in

pyrazolo[1,5-*a*]pyrimidine derivatives the most active compound was the 3-((4-acetylphenyl)diazenyl)-2,5-diamino-7-(4-chlorophenyl) pyrazolo[1,5-*a*]pyrimidine-6-carbonitrile **7a**, with C=O group, IC<sub>50</sub> = 3.25  $\mu$ M; while its analog **7d** showed poor anticancer activity (IC<sub>50</sub> = 906.6  $\mu$ M). The activity of the pyrazolo [1,5-*a*]pyrimidine **7a** displayed a 5 fold decrease upon replacement of the 4-Cl-phenyl in position 7 with the 2,3-(OCH<sub>3</sub>)<sub>2</sub>Ph moiety as in **7c** (IC<sub>50</sub> = 15.4  $\mu$ M). It is worth mentioning that the pyrazolopyrimidines **7a, c** bearing a C=O group were by far much more effective antiproliferative activity than their counterparts **7d, f** containing C=NNH<sub>2</sub> (IC<sub>50</sub> = 3.25, 15.4, 906.6, 871.9  $\mu$ M, respectively).

Additionally, it was found that 7-Amino-N-(4-chlorophenyl)-6-cyano-5-(4-fluorophenyl)-2-(4-methoxy-phenyl-amino) pyrazolo[1,5-*a*]pyrimidine-3-carboxamide prepared by Hassan *et al.*[27] is slightly potent than **7a**, this may be due to the presence of a primary amine in **7a** while the other compound has lipophilic secondary amine.

On the contrary, pyrazolopyrimidines 5d, e, carrying C=NNH<sub>2</sub>, displayed more activity against human breast cancer MCF-7 cell line (IC<sub>50</sub> = 40.2, 28.2 μM) than their analogs 5a, b (IC<sub>50</sub> = 1083, 181 μM respectively).

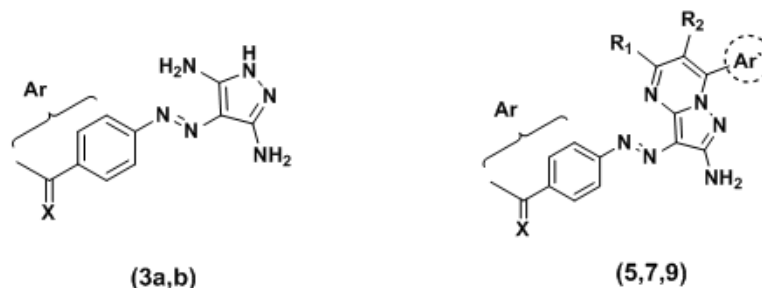
Moreover, poor activity was elicited by pyrazolopyrimidines 9a, b.

#### Effect of 7a on cell cycle arrest in MCF-7 cells

The most active compound 7a was selected for further study due to its effect on cell cycle progression in the MCF-7 cell line. The MCF-7

cells were incubated with GI<sub>50</sub> concentration of compound 7a for 24 h and its effect on the normal cell cycle profile was analyzed. Flow cytometric analysis was performed to measure the effect of compound 7a on induction of cell cycle. As shown in fig. 2, the cells in S phase in the MCF-7 control group accounted for about 23.59%, while after cells treated with compound 7a, the ratio was approximately 32.66%. This shows that the cells were arrested in the S phase. Such increase was accompanied by a reduction of cells at the G<sub>2</sub>/M phase of the cell cycle, which resulted in an interference with the normal cell cycle distribution of this cell line.

**Table 1: IC<sub>50</sub>'s of the tested compounds against human breast cancer cells (MCF-7)**



Compound	R1	R2	Ar'	X	ic50(mean±SD)
3a	-	-	-	O	26.2±0.70
3b	-	-	-	NNH <sub>2</sub>	1083.3±28.8
5a	Ph	H	4-ClPh	O	1083.3±28.8
5b	Ph	H	4-CH <sub>3</sub> Ph	O	181±1
5c	Ph	H	3,4,5(OCH <sub>3</sub> ) <sub>3</sub> Ph	O	1250±50
5d	Ph	H	4-ClPh	NNH <sub>2</sub>	40.2±0.64
5e	Ph	H	4-CH <sub>3</sub> Ph	NNH <sub>2</sub>	28.2±0.68
5f	Ph	H	3,4,5(OCH <sub>3</sub> ) <sub>3</sub> Ph	NNH <sub>2</sub>	97.5±0.51
7a	NH <sub>2</sub>	CN	4-ClPh	O	3.25±0.52
7b	NH <sub>2</sub>	CN	4-OCH <sub>3</sub> Ph	O	948±7.2
7c	NH <sub>2</sub>	CN	2,3-(OCH <sub>3</sub> ) <sub>2</sub> Ph	O	15.4±0.51
7d	NH <sub>2</sub>	CN	4-ClPh	NNH <sub>2</sub>	906.6±6.1
7e	NH <sub>2</sub>	CN	4-OCH <sub>3</sub> Ph	NNH <sub>2</sub>	1243.3±40.4
7f	NH <sub>2</sub>	CN	2,3-(OCH <sub>3</sub> ) <sub>2</sub> Ph	NNH <sub>2</sub>	871.9±7.5
9a	NH <sub>2</sub>	COOEt	H	O	1516±28.8
9b	NH <sub>2</sub>	CN	H	NNH <sub>2</sub>	1196.6±15.2

IC<sub>50</sub>: Compound concentration required to inhibit the cell viability by 50%, SD= standard deviation; each value is the mean of three values.

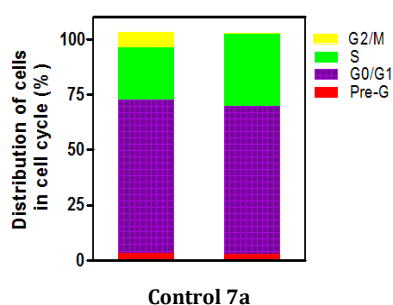


**Fig. 2: Bar chart shows the percentage of MCF7 cells at each phase of cell cycle in control cells and cells treated with compound 7a**

#### QSAR studies

Equation one represents our best-performing QSAR model; Fig.3 shows the corresponding scatter plots of the experimental versus estimated bioactivity values for the training set compounds, against MCF-7 cell line. Interestingly, the predicted anti-tumor activity by the QSAR model was very close to the experimentally observed, indicating that these models can be applied for prediction of more effective hits having the same skeletal framework as that of the potent antitumor compound.

Equation 1 represents the best performing QSAR model for the activity against MCF-7 cell line.

$$-\log IC_{50} = -4.2305 + 0.30198 ES\_Sum\_dsN + 0.81231 Dipole\_mag + 0.14287 Jurs\_WNSA\_3$$

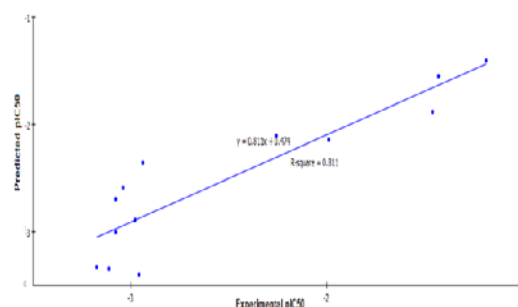


**Fig. 3: Predicted versus experimental PIC50 values of the training set compounds against human breast cancer cell line (MCF-7) according to equation 1 (r<sup>2</sup>= 0.811)**

According to equation 1, the QSAR model was represented graphically by scattering plots of the experimental versus the

predicted bioactivity values  $-\log IC_{50}$  for the training set compounds as shown in fig. 3. The method used to build the model was Least-Squares,  $r^2 = 0.811$ ,  $r^2$  (adj) = 0.748,  $r^2$  (pred) = 0.604, where  $r^2$  (adj) is  $r^2$  adjusted for the number of terms in the model;  $r^2$  (pred) is the prediction  $r^2$ , equivalent to  $q^2$  from a leave-1-out cross-validation.

Moreover, the MLR model developed in this work which involves three descriptors, reveals that the anticancer activity should correlate directly proportional with ES\_Sum\_dsN, Dipole\_mag, Jurs\_WNSA\_3. Additionally, the anticancer activities of the synthesized compounds are affected by these descriptors.

#### QSAR validation

Robustness of the established QSAR model was verified by using: Leave-one-out (LOO) internal validation  $r^2 = 0.811$ . Cross-validation was also employed where  $q^2$ , which is equivalent to  $r^2$  (pred) was 0.94. In addition, validation was employed by measuring the residuals between the experimental and the predicted activities of the training set c. f. supplementary material Furthermore, compounds 7a, 5d, 3b were used as statistical outliers where their  $pIC_{50}$  values were -0.511, -1.609, -3.041 respectively, their expected  $pIC_{50}$  values were -0.388, -1.963, -2.811 respectively with residuals -0.123, 0.354, -0.230 respectively. The 2D QSAR studies, MLR model, showed high correlative and predictive abilities. Furthermore, the generated QSAR models performed to explore the structural features required for the observed antitumor property, revealed that the biological activities were influenced by the molecular descriptors: ES\_Sum\_dsN, Dipole\_mag, Jurs\_WNSA\_3 of the synthesized compounds.

#### Pharmacophore modeling

It produced ten top-scored hypotheses based on the activity values of the training set molecules. The best ten hypotheses contained four

features: HBD, HBA, H and RA. Hypo1 consisted of two HBA and one RA, as shown in Fig. 4 with constraint distances and angles between its features as described in (table 2), it also established the highest cost difference (118.89), lower errors (86.12), best correlation coefficient (0.86), maximum fit value (8.04) and lowest root mean square RMS of (2.45).

This pharmacophore hypothesis generated was developed with a total cost value of (103.78), null cost value of (222.67), and fixed cost value of (52.98). The Fixed total cost was dependent on a summation of the cost components: weight cost, error cost and configuration cost.

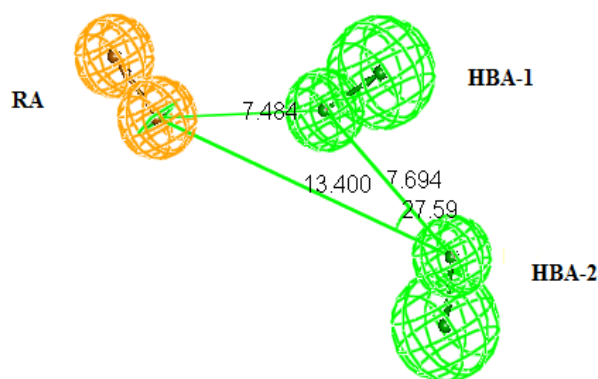


**Fig. 4: Constraint distances and angles between features of the generated top pharmacophore model with the features considered hydrogen bond acceptors (HBA1 & HBA2) colored in green, and aromatic ring (RA) colored in orange**

**Table 2: Constraint distances and angles between features of the generated top pharmacophore model**

Constraint distances (Å)	Constraint angles (°)
(HBA1-HBA2): 7.694	HBA1, HBA2, RA: 27.59
(RA-HBA1): 7.484 (RA-HBA2): 13.400	

Two key values were used for cost analysis: one is the difference between the fixed and null costs and another one is the difference between null and total cost (cost difference). The fixed cost represents a cost of the ideal theoretical hypothesis, which could absolutely predict the activity of compounds in the training set with the lowest deviation while null cost represented the cost of hypothesis with no features that estimate every activity to be the average activity. The difference between these two costs should be greater than or equal 70 bits to show 98% statistical significance of the model. The cost difference should be greater than 60 bits to represent a true correlation data.

Higher cost difference and correlation value with low RMS and error values have been observed for Hypo1 when compared with the other hypotheses. Hence, Hypo1 was selected as the best hypothesis and employed for further analyzes, Fig. 4 shows, the Hypo1 chemical features with its geometric parameters. The most active compound 7a in the training set a ligned in Hypo1 was shown in fig. 5. To verify, the prediction accuracy of Hypo1, Hypo1 was also able to estimate the activities of compounds in their own activity ranges. The experimental and estimated activities by Hypo1 for 16 training set compounds are shown in (table 3).

The parameters were computed by regression analysis using the relationship of fit geometric value versus the activity. The better the geometric fit the greater the activity prediction of the compound. The fit function checks if the feature is mapped. It also contains a distance term, which measures the distance separating the feature on the molecule from the centroid of the feature in the pharmacophore hypothesis. Both terms are used to calculate the fit geometric value.

The Fischer validation confidence level chosen is 98%, and the best-generated pharmacophore significance was 82%. Further evaluation of the generated pharmacophore models was based on the

correlation coefficient, which was found to be 0.86 that indicate the capability of the pharmacophore model to predict the activity of the training set compounds.

In addition to cost analysis and Fischer validation, the pharmacophore model was validated through activity prediction of the synthesized structures as a training set. The predicted activities through the pharmacophore model are represented in (table 3) as well as their fit values.

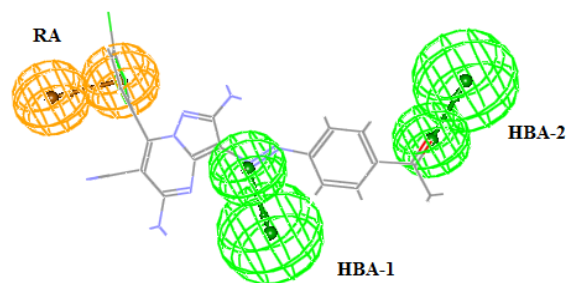


**Fig. 5: The best-generated pharmacophore hypothesis with the features considered hydrogen bond acceptors (HBA1 and HBA2) colored in green, ring aromatic (RA) colored in orange and the synthesized structure 7a fitted in the pharmacophore with fit value 7.24**

#### Validation of pharmacophore modeling

One of the significant methods in pharmacophore generation is validating the hypothesis. The generated hypotheses were mainly validated to check whether the best hypothesis selected the active

compounds during the screening process such as the percentage of active compounds picked from the dataset, correlation between the predicted and estimated values of the set test along with its efficiency in reducing true negatives and false positives. The selected Hypo1 was validated using the following methods; cost analysis, activity prediction, Fischer validation test.

HypoGen selects the best hypotheses by applying a cost analysis. The overall cost of each hypothesis is calculated by summing three

cost factors: a weight cost, an error cost, and a configuration cost. HypoGen also calculates two theoretical costs, the null and fixed costs that can be used to determine the significance of the selected hypothesis.

The cost values of the optimized hypothesis should lie somewhere between these two costs. A larger difference between the fixed and null costs than that between the fixed and total costs signifies the quality of a pharmacophore model.

**Table 3: Fit values and estimated activities for the synthesized compounds mapped with the generated 3D-pharmacophore model**

Compound	Predicted activity (IC <sub>50</sub> μM)	Experimental activity (IC <sub>50</sub> , mean) μM	Fit value
3a	361.22	26.2	5.33
3b	1633.23	1083.3	4.67
5a	396.08	1083.3	5.29
5b	190.64	181	5.60
5c	382.93	1250	5.30
5d	55.19	40.2	6.14
5e	32.79	28.2	6.37
5f	484.64	97.5	5.20
7a	4.41	3.25	7.24
7b	417.51	948	5.26
7c	13.85	15.4	6.74
7d	705.06	906.6	5.04
7e	674.15	1243.3	5.06
7f	820.41	871.9	4.97
9a	369.89	1516.6	5.32
9b	1002.31	1196.6	4.88

IC<sub>50</sub>: Compound concentration required inhibiting the cell viability by 50%; each value is the mean of three values.

The closer the cost value to the fixed cost and the further away it is from the null cost, the more statistically significant the hypothesis is believed to be.

Fischer validation is another approach for pharmacophore model validation. This validation method checks the correlation between the chemical structures and biological activity. This method generates pharmacophore hypothesis using the same parameters as those used to develop the original pharmacophore hypothesis by randomizing the activity data of the training set compounds. The purpose of this study was not only to construct the pharmacophore model to predict the estimated activity of the compounds but also to employ the hypothesis on virtual screening to search novel scaffolds. In this work, we have built 3D pharmacophore models from 16 newly synthesized compounds and the best quantitative pharmacophore model, Hypo1, consisted of three features like two HBA and one RA.

For predicting activity, the correlation coefficient of Hypo1 was 0.86, suggesting a good predictive power of the hypothesis for the majority of antitumor actives.

From the overall analysis, we conclude that the Hypo1 pharmacophore could be used as the fast and accurate tool to assist discovery of novel anticancer agents.

## CONCLUSION

In an effort to develop potent anticancer agents, pyrazoles 3a, b and pyrazolo[1,5-*a*]pyrimidines 5a-f, 7a-f, 9a, b were designed and synthesized. Anti-proliferative activity of the newly synthesized compounds was examined against MCF-7 breast cancer using MTT technique. Compound 7a was found to be the most active member against MCF-7 breast cancer (IC<sub>50</sub> = 3.25 μM). Further biological assessment of 7a using flow-cytometric analysis, revealed that it induced cell cycle arrest at S phase. 3D-QSAR pharmacophore modeling afforded a hypothesis with three chemical features: 2HBA, 1RA. QSAR studies showed good predictive and statistically significant descriptor model with  $r^2$  0.811. The most important descriptors in the QSAR equation were ES\_Sum\_dsN, Dipole\_mag, Jurs\_WNSA\_3. The combination of 3D-pharmacophore modeling and QSAR provides as an effective technique for understanding the

observed pharmacological properties and thus could be adopted for developing effective lead structures.

## ACKNOWLEDGEMENT

The authors are grateful to Pharmacology Department, Faculty of Pharmacy, Al-Azhar University, Cairo, Egypt for carrying out the anticancer screening.

## CONFLICT OF INTERESTS

The authors confirm that this article content has no conflicts of interest

## REFERENCES

- Jemal A, Siegel R, Ward E, Murray T, Xu J, Thun MJ. Cancer statistics. *CA Cancer J Clin* 2007;57:43-66.
- David ET. Chemistry and pharmacology of anticancer drugs. 1st ed. Taylor and Francis group editor. New York: CRC PRESS; 2007.
- Keshtgar M, Davidson T, Pigott K, Falzon M, Jones A. Current status and advances in the management of early breast cancer. *Int J Surg* 2010;8:199-202.
- Maughan KL, Lutterbie MA, Ham PS. Treatment of breast cancer. *Am Fam Physician* 2010;81:1339-46.
- Nahren MM, Nanda G. An efficient tool for identifying inhibitors based on 3D-QSAR and docking using feature-shape pharmacophore of biologically active conformation-A case study with CDK2/Cyclin A. *Eur J Med Chem* 2008;43:2807-18.
- Bronson J, Dhar M, Ewing W, Lonberg N. Chapter thirty-one – to market, to market-2011. *Annu Res Med Chem* 2012;47:548.
- Ruth PF, Pilar G, José E. A review of recent progress (2002-2012) on the biological activities of pyrazoles. *Arkivoc* 2014;2:233-93.
- Bronson J, Dhar M, Ewing W, Lonberg N. *Annu Res Med Chem*. 1st ed. Elsevier Inc; 2012.
- Berger DM, Torres N, Dutia M, Powell D, Ciszewski G, Gopalsamy A, *et al.* Non-hinge-binding pyrazolo[1,5-*a*]pyrimidines as potent B-Raf kinase inhibitors. *Bioorg Med Chem Lett* 2009;19:6519-23.

10. Williamson DS, Parratt MJ, Bower JF, Moore JD, Richardson CM, Dokurno P, *et al.* Structure-guided design of pyrazolo[1,5-a]pyrimidines as inhibitors of the human cyclin-dependent kinase. *J Bioorg Med Chem Lett* 2005;15:863-7.
11. Li R, Ellen RL, Alex JB, Victoria D, Susan LG, Jonas Grina, *et al.* Potent and selective pyrazolo[1,5-a]pyrimidine based inhibitors of B-Raf(V600E) kinase with favorable physicochemical and pharmacokinetic properties. *Bioorg Med Chem Lett* 2012;22:1165-8.
12. Al-Sehemi AG, Irfan A, Fouda AM. Synthesis, characterization and density functional theory investigations of the electronic, photophysical and charge transfer properties of donor-bridge-acceptor triaminopyrazolo[1,5-a]pyrimidine dyes. *Spectrochim Acta Part A* 2013;111:223-9.
13. Khurana JM, Kiran D, Susruta M. An efficient 1,3-allylic carbonyl transposition of chalcones. *Monatsh Chem* 2009;140:69-72.
14. Xiang-Shan W, Zhao-Sen Z, Yu-Ling Li, Da-Qing S, Shu-Jiang Tu, Xian-Yong W, *et al.* Simple procedure for the synthesis of aryl methylene malononitrile without a catalyst. *Synth Commun* 2005;35:1915-20.
15. Claudia R, Renate D, Hans J, Heinz G. Possible rearrangements during the synthesis of di-and trisubstituted pyrazoles. *Montash Chem* 1998;129:1313-8.
16. Mosmann T. Rapid colorimetric assay for cellular growth and survival: application to proliferation and cytotoxicity assays. *J Immunol Methods* 1983;65:55-63.
17. Dominic AS, Robert HS, Kenneth DP, Anne M, Siobhan T, Thomas HN, *et al.* Evaluation of a soluble tetrazolium/formazan assay for cell growth and drug sensitivity in culture using human and other tumor cell lines. *Cancer Res* 1988;48:4827-33.
18. Adel SG, Jacek S, Nasser SM, Hanaa F. Synthesis and QSAR study of novel cytotoxic spiro[3H-indole-3,20(10H)-pyrrolo[3,4-c]pyrrole]-2,3',5'(1H,2'aH,4'H)-triones. *Eur J Med Chem* 2012;47:312-22.
19. Saleh NM, Ammar YA, Micky JA, Abbas HA, EL-Gaby MS. Novel synthesis and antimicrobial investigation of pyrazolo[1,5-a]pyrimidine and pyrazolotriazine containing piperidinyl sulfone moiety. *Indian J Chem* 2004;43B:2195-202.
20. Krystof V, Cankar P, Frysová I, Slouka J, Kontopidis G, Dzubák P, *et al.* 4-Arylazo-3,5-diamino-1H-pyrazole CDK inhibitors: SAR study, crystal structure in complex with CDK2, selectivity, and cellular effects. *J Med Chem* 2006;49:6500-9.
21. El-Shafei A, Fadda AA, Khalil AM, Ameen TAE, Badria FA. Synthesis, antitumor evaluation, molecular modeling and quantitative structure-activity relationship (QSAR) of some novel arylazopyrazolo diazine and triazine analogs. *Bioorg Med Chem* 2009;17:5096-105.
22. Karci F, Demircal A. Synthesis of disazopyrazolo[1,5-a]pyrimidines. *Dyes Pigm* 2007;74:288-97.
23. Fadda AA. Synthesis of some new arylazothiophene and arylazopyrazole derivatives as antitumor agents. *Pharmacol Pharm* 2012;3:148-57.
24. Tsai PC, Wang IJ. A facile synthesis of some new pyrazolo[1,5-a]pyrimidine heterocyclic disazo dyes and an evaluation of their solvatochromic behavior. *Dyes Pigm* 2007;74:578-84.
25. Dawane BS, Konda SG, Zangade SB. Design, synthesis, and characterization of some novel pyrazolo[1,5-a]pyrimidines as potent antimicrobial agents. *J Heterocycl Chem* 2010;47:1250-4.
26. Elfahham HA, Elgemeie GH, Ibraheim YR, Elnagdi MH. Studies on 3,5-diaminopyrazoles: new routes for the synthesis of new pyrazoloazines and pyrazoloazoles. *Liebigs Ann Chem* 1988;8:819-22.
27. Hassan AS, Hafez TS, Osman SA, Ali MM. Synthesis and *in vitro* cytotoxic activity of novel pyrazolo[1,5-a]pyrimidines and related Schiff bases. *Turk J Chem* 2015;39:1102-13.